DOI: 10.1002/ejic.200600853

Syntheses and Characterization of Molybdenum/Zinc Porphyrin Dimers Bridged by Aromatic Linkers

Sai-Nan Song,[a] Dong-Mei Li,*[a,b] Jun-Feng Wu,[a] Chang-Fu Zhuang,[a] Hong Ding,[a] Wen-Bo Song,[a] Li-Feng Cui,[a] Geng-Zhen Cao,[a] and Guo-Fa Liu[a]

Keywords: Porphyrinoids / Heteronuclear complexes / Bridging ligands / Molybdenum / Zinc / Electrochemistry

Two new heterobinuclear porphyrin dimers, namely [{$Mo^{VI}O_2$}-DBPA-Zn] (**1**; H_4DBPA = *N*,*N*′-dibenzylidenebis-[4-(10,15,20-triphenyl-21*H*,23*H*-porphin-5-yl)phenylamine]) and [{$Mo^{VI}O_2$}-PBDA-Zn] (**2**; H_4PBDA = *N*,*N*′-bis[4-(10,15,20-triphenyl-21*H*,23*H*-porphin-5-yl)phenyl]-1,3-benzenedicarboxamide), have been synthesized. These bis-(porphyrin)s were obtained by treating 5-(*p*-aminophenyl)-10,15,20-triphenylporphyrinatomolybdenum and -zinc with benzene-1,4-dicarboxaldehyde or benzene-1,3-dicarboxylic acid. They have been characterized by UV/Vis, IR, X-ray photoelectron, luminescence, and ^{1}H NMR spectroscopy, and their TG-DTA behavior and molar conductances have also been determined. Th *cis*-dioxomolybdenum(VI) unit in these complexes is contained in one of the porphyrin moieties and zinc(II) ion is tetracoordinated in the other. Their electrochemical properties have also been investigated in detail.

Introduction

Large π-conjugated macrocyclic systems like porphyrins are fascinating functional materials with high chemical and thermal stability whose photophysical and photochemical properties can be finely tuned by structural modifications involving the substitution of functional groups or different metal coordination.[1–3] Among the many porphyrins and metalloporphyrin complexes, dimeric and oligomeric porphyrins with extensive electronic delocalization have attracted increasing interest due to their potential applications in molecular electronics and photonics, which range from light-emitting diodes,[4] nonlinear optical (NLO) materials,[5] information storage materials,[6] photovoltaic cells,[7–9] chemical sensors,[10] biomimetic systems,[11,12] photosensitizers in photodynamic therapy,[13,14] and so forth. Optional linkages connecting monomeric porphyrin rings would allow the spatial configuration of porphyrins to be adjusted, thereby altering the sizes and shapes of the porphyrinato cavities. Generally speaking, three kinds of linkages are observed in porphyrin dimers and oligomers: (1) a flexible spacer such as a variable-length hydrocarbon or one containing mixed atoms;[15] (2) a rigid spacer such as diphenylanthracene, diphenylene, or *o*-phenylene;[16] (3) a direct *meso*-linked dimer or oligomer.[17,18]

Bis(porphyrin) complexes containing different metal ions, for example Mo/Os, W/Ru, Sn/Mo, and Gd/Co,[19–22] afford heterometallic dimers with extremely interesting magnetic or bifunctional catalytic properties compared with homometallic bis(porphyrin)s (Co/Co, Pd/Pd).[23,24] Molybdenum exhibits oxidation states from +2 to +6 in its porphyrin complexes[25–27] and several studies have demonstrated that high-valent molybdenum porphyrin complexes with *trans*-diperoxo, *cis*-dioxo, and *cis*-oxo-peroxo groups exhibit good oxygen transport activity in vivo and high catalytic activity toward oxygenation reactions.[28–31] We are currently focussing on heterometallic bis(porphyrin)s containing molybdenum in a high oxidation state (+6), and in this paper we report the syntheses, spectral characterization, and electrochemical properties of two new molybdenum–zinc porphyrin dimers, namely [{$Mo^{VI}O_2$}-DBPA-Zn] (**1**; H_4DBPA = *N*,*N*′-dibenzylidene-bis[4-(10,15,20-triphenyl-21*H*,23*H*-porphin-5-yl)phenylamine]) and [{$Mo^{VI}O_2$}-PBDA-Zn] (**2**; H_4PBDA = *N*,*N*′-bis[4-(10,15,20-triphenyl-21*H*,23*H*-porphin-5-yl)phenyl]-1,3-benzenedicarboxamide) that contain a *p*-bis(Schiff base)phenyl or a *meta*-diimidophenyl as a linking spacer.

Results and Discussions

Synthesis of the Complexes

Bis(porphyrin)s can be obtained by self-assembly of monomeric porphyrins through van der Waals or π–π interactions.[32–34] Herein, two kinds of linkers have been chosen, one of which is formed by simple acylation of a diacid and 5-(*p*-aminophenyl)-10,15,20-triphenylporphyrin [5-(*p*-NH_2)-TPP] whilst the other is obtained by direct reaction of a dialdehyde and 5-(*p*-NH_2)TPP. Two strategies to insert dif-

[a] College of Chemistry, Jilin University,
Jiefang Road 2519, Changchun 130023, P. R. China
[b] Nanoscale Physics & Devices Laboratory, Institute of Physics, Chinese Academy of Sciences,
Beijing 100080, P. R. China
E-mail: dmli@aphy.iphy.ac.cn

ferent metal ions into the bis(porphyrin) cavities have also been followed, both of which gave satisfactory results. One approach involves the reaction of one molar equivalent of the mononuclear porphyrin complexes [{5-(*p*-NH_2)TPP}-Zn] (**3**) and [{5-(*p*-NH_2)TPP}$Mo^{VI}O_2$] (**4**) with the bridge-linking reagents (see Scheme 1).

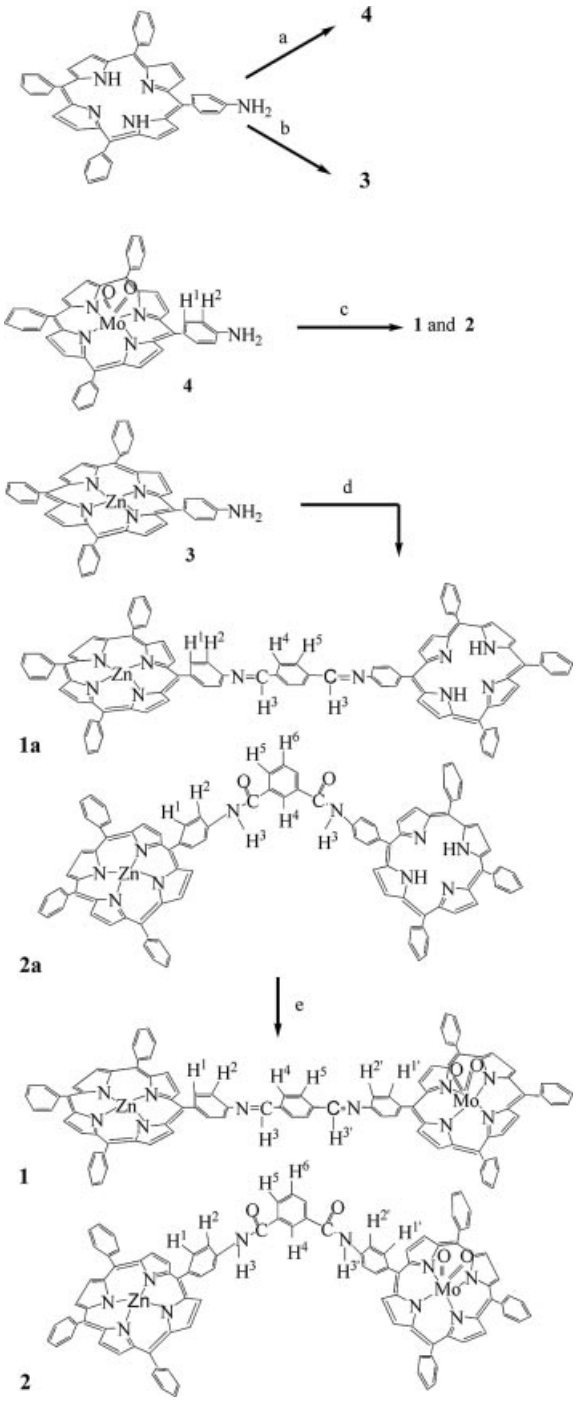

Scheme 1. a: $Mo(CO)_6$, 1,2,4-trichlorobenzene; b: $Zn(OAc)_2{\cdot}2H_2O$, dmf; c: **3** and benzene-1,4-dicarbaldehyde in dmf (to yield **1**) or benzene-1,3-dicarboxylic acid in dmf (to yield **2**); d: 5-(*p*-NH_2)TPP and benzene-1,4-dicarbaldehyde (to yield **1a**) or benzene-1,3-dicarboxylic acid in dmf (to yield **2a**); e: $Mo(CO)_6$, 1,2,4-trichlorobenzene.

The progress of the reaction was monitored by recording the UV/Vis absorption spectra. Completion of the reaction was indicated by a change in the relative intensities of the bands centered at about 555 and 595 nm and the appearance of a new band at around 450 nm. However, this reaction also produces several by-products and therefore requires further purification steps. Follow-up experiments revealed that adjusting the molar ratio (1:1) and the charging sequence of the starting materials improves the yield.

The second synthetic strategy consists of two steps: preparation of the mono-zinc bis(porphyrin) complexes **1a** and **2a**, and subsequent treatment of **1a**, **2a** with $Mo(CO)_6$ to give the Mo/Zn compounds.[35] This method produces fewer by-products, although the yield of compound **2** is low, presumably due to the cleavage of the imido linkage at higher temperatures.

Composition of the Complexes

The heterobimetallic porphyrin complexes **1** and **2** were isolated as stable, purple, microcrystalline solids, although recrystallization from different organic solvents failed to give crystals suitable for an X-ray diffraction study. This lack of crystals led us to seek alternative ways to deduce the possible coordination modes of the central metals. The formulations [{$Mo^{VI}O_2$}-DBPA-Zn] (**1**) and [{$Mo^{VI}O_2$}-PBDA-Zn] (**2**) are proposed based on the elemental analyses, mass spectra, molar conductance, and XPS (as well as spectral and electrochemical characteristics, see below). First, the elemental analyses of **1**, **2**, and **4** are consistent with their respective compositions, thus implying that the *cis*-dioxomolybdenum unit has been successfully inserted into the porphyrinato rings. Second, the mass spectrum of [{5-(*p*-NH_2)TPP}$Mo^{VI}O_2$] (**4**) shows the molecular ion peak at *m*/*z* 757 $[M + 2]^+$ and the base peak at *m*/*z* 741 $[M + 2 - O]^+$. The MALDI-TOF spectrum of **1** matches the calculated abundance, thereby confirming its elemental composition and the dimeric structure (peaks at *m*/*z* 736.0 and 692.1 attributable to [{5-(*p*-NH_2)TPP}$Mo^{VI}O$] and [{5-(*p*-NH_2)TPP}Zn], respectively). This evidence suggests that four nitrogen atoms from the porphyrin β-pyrroles are chelated to the molybdenum atom with the two oxo ligands adopting a *cis* configuration on the same side of the porphyrin ring. Third, the molar conductance values in 1.0×10^{-3} M chloroform solution at 25 °C are 0.028, 0.039, 0.022, 0.030, 0.030, and 0.033 $\Omega^{-1}\,cm^2\,mol^{-1}$ for dimers **1**, **2**, **1a**, and **2a** and monomers **3** and **4**, respectively, thus indicating that all these porphyrin complexes exhibit nonelectrolytic behavior.[36] Finally, X-ray photoelectron spectroscopy (XPS) was employed to determine the oxidation state of the molybdenum atoms in the Mo/Zn dimers. Mo $3d_{5/2}$ binding energies of 232.3 eV for compound **1** and 232.6 eV for compound **2** were observed, which suggests that the valence state of molybdenum atom in the two compounds is +6.[37,38] Thus, on the basis of the data available, it is assumed that the zinc(II) ion in these Mo/Zn dimers is tetracoordinate to the four pyrrole nitrogens from one

porphyrin ring while the molybdenum(VI) atom is hexacoordinate to the other porphyrin ring with the two oxygen atoms located in a *cis* position, as illustrated in Scheme 1.

No axial ligand is present in the porphyrinatozinc subunits of **1** and **2** as two important effects of axial ligands are not observed.[39–41] Thus, the absorption spectrum of [{5-(*p*-NH_2)TPP}Zn] (**3**) was obtained in chloroform, a poorly coordinating solvent, which means that no solvent molecule is ligated to the zinc ion. The other complexes **1a**, **2a**, **1**, and **2** did not show a red shift of their Soret bands relative to **3**. Similarly, no change in the relative intensities of the bands at around 550 and 590 nm is observed (see UV/vis section below).[39] This kind of coordination mode for two metal centers is different from the known anthracene-bridged Mo/Zn porphyrin dimer with an oxomolybdenum(V) unit[42] and other zinc porphyrin complexes with different axial ligands.[43] In fact, some mixed-metal Zn/M bis(porphyrin) complexes (M = Pd, Zn, H_2) possess a similar coordination mode, mainly due to the different synthetic methodologies.[15,44,45]

Infrared Spectra

The mono-zinc and heterometallic Mo/Zn bis(porphyrin) complexes give complicated IR spectra. However, they display characteristic IR absorptions that are helpful for identifying the functional groups. For example, the mono-zinc bis(porphyrin) **1a** shows strong stretching bands at 1659 and 1628 cm^{-1} for the C=N bond of the Schiff base, while the mono-zinc bis(porphyrin) **2a** exhibits intense bands at 1652 and 1635 cm^{-1} due to the symmetric C=O stretching vibrations of the imido groups. Upon coordination of the mono-zinc bis(porphyrin)s to the molybdenum atom these bands shift to higher wavenumbers (1697 and 1651 cm^{-1} for **1** and 1652 cm^{-1} for **2**). This shift is primarily associated with the increasing asymmetry of the molecule as a whole. Furthermore, additional bands at 910 and 951 cm^{-1} are observed in **1** and **2**, respectively, due to the Mo=O stretching vibrations. Similar bands have also been found in other molybdenum porphyrin complexes such as [O=Mo(TPP)OH] and [O=Mo(TPP)X] [X = OMe, OEt, O*i*Pr, O*t*Bu].[43]

UV/Vis Spectra

The bis(porphyrin)s with different bridges exhibit typical UV/Vis spectra in chloroform in the visible and near-ultraviolet regions. Their maximum absorption wavelengths are listed in Table 1 along with the corresponding monoporphyrin compounds.

As can be seen in Figure 1 (a) and Table 1, Mo/Zn bis(porphyrin) complexes **1** and **2** show very similar absorptions and the mono-zinc bis(porphyrin) complexes **1a** and **2a** also give quite similar absorptions. Apparently, the two different linkers do not significantly influence the UV/Vis absorptions of the bis(porphyrin)s. The Mo/Zn dimers give two Soret absorptions at around 340 and 424 nm, which suggest that both Mo^{VI} and Zn ions can be introduced into the porphyrin rings since the absorptions in the ranges 330–340 nm and 420–425 nm are much closer to those found in the monomeric complexes **4** and **3**, respectively. Figure 1 (b) shows the UV/Vis spectra of **3** and **4** as well as their superposition. It is to be expected, and is indeed observed, that the overlapping peaks of **3** and **4** should be similar to those of **1** and **2** (there is no obvious shift in the Soret bands). This result strongly suggests that no axial ligand (e.g., ethanol) is coordinated to the Zn^{2+} ion.

^{1}H NMR Spectra

Further confirmation of the identity of **1** and **2** was provided by their ^{1}H NMR spectra. We collected the ^{1}H NMR spectroscopic data of mono-zinc bis(porphyrin)s **1a** and **2a** and Mo/Zn porphyrin dimers **1** and **2** in $CDCl_3$. A weak signal at δ = –2.75 ppm was observed for **1a** and **2a** due to the pyrrolic nitrogen protons. This signal disappears after the four pyrrolic nitrogens become coordinated to the molybdenum atom. On the other hand, the broad singlet at δ = 4.11 ppm due to the amino protons in **4** disappears after

Table 1. UV/Vis spectra of the ligands and complexes.

Compounds	λ_{max} [nm] (ε [10^3 M^{-1} cm^{-1}]) Soret band	Q bands				Ref.
5-(*p*-NH_2)TPP	426 (263.4)	518 (28.7)	554 (15.8)	592 (9.1)	648 (7.6)	this work
3	428 (277.6)		554 (19.8)	596 (7.7)		this work
4	341 (50.7)	459 (66.5)			647 (14.9)	this work
1a	429 (269.3)	517 (18.3)	554 (27.3)	595 (12.5)	648 (4.9)	this work
2a	428 (277.1)	519 (17.2)	554 (26.0)	594 (11.8)	650 (4.9)	this work
1	337 (62.4) 425 (285.6)	454 (68.1)	552 (29.0)	593 (13.4)	625 (7.6)	this work
2	340 (59.8) 424 (293.8)	458 (89.5)	553 (24.1)	590 (14.5)	626 (9.7)	this work
5[a]	341 (81.1) 414 (249)	458 (41.4)	545 (16.8)	575 (16.9)	598 (4.7)	[42]
6[b]	425 (214)	487 (4.6)	535 (15.2)	562 (11)		[44]
7[c]	453 (182)	540 (3.5)	581 (15.9)	620 (10.9)	540 (3.5)	[43]

[a] **5** = (DPA)[$Mo^{V}O$(OMe)][Zn(MeOH)] (DPA = 1,8-bis[5-(2,8,13,17-tetraethyl-3,7,12,18-tetramethylporphyrinyl)]anthracene). [b] **6** = [MoO_2(TTP)] (TTP = 5,10,15,20-tetra-*p*-tolylporphyrin). [c] **7** = [MO(TPP)OEt] (TPP = 5,10,15,20-tetraphenylporphyrin).

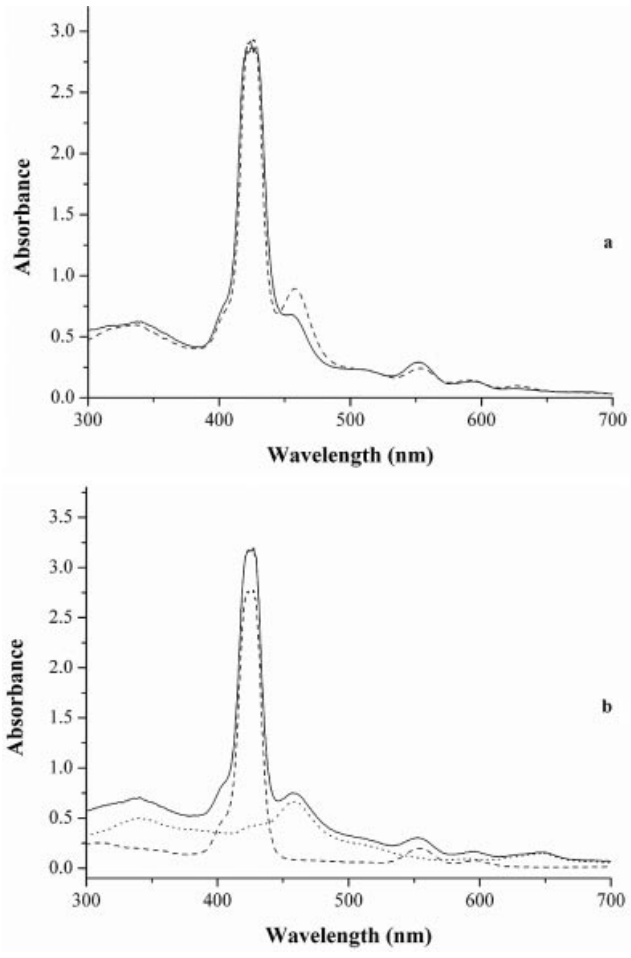

Figure 1. UV/Vis spectra of a series of porphyrin complexes in chloroform at room temperature: (a) Mo/Zn bis(porphyrin) complexes **1** (solid line) and **2** (dashed line); (b) [{5-(*p*-NH_2)TPP}Zn] (dashed line), [{5-(*p*-NH_2)TPP}$Mo^{VI}O_2$] (dotted line), and their difference spectrum (solid line).

reaction with the linkers. New broad singlets at around δ = 10.15 ppm due to the protons of the Schiff base [C(*H*)=N] are observed in **1a** and **1**, whereas a new resonance at around δ = 10.30 ppm is found for the amide proton [C(O)-N*H*] in **2a** and **2**. Mono-substitution on the phenyl rings impose an effective C_s symmetry on the metalloporphyrin moiety, which leads to a splitting of the pyrrole resonances. This tendency is also observed here, where the pyrroles adjacent to the 5-*meso* position bear non-equivalent pairs of protons (see Experimental Section). Besides, **1a** shows a singlet at δ = 8.23 ppm due to the *ortho* protons, two doublets at δ = 7.89 and 7.77 ppm due to the *para* and *meta* protons of the *meso*-substituted phenyls, respectively, and two doublets at δ = 8.08 and 7.63 ppm due to the 5-*meso*-substituted phenyl. For the corresponding Mo/Zn complex **1**, these signals are observed at δ = 8.24, 7.86, 7.76, 8.07, and 7.69 ppm, respectively. Obviously, these values are too similar to allow any distinctive differences between the two compounds to be determined. Similar phenomena are observed for **2a** and **2**. As regards the Schiff base linker, **1a** shows two doublets at δ = 7.57 and 7.53 ppm attributable to the phenyl protons, and these resonances are observed at δ = 7.53 and 7.50 ppm for **1**. For the imido linkage, **2a** shows signals at δ = 8.01 and 7.95 ppm due to the phenyl protons while signals at δ = 7.99, 7.88, and 7.46 ppm are observed for **2**. Therefore, the ring current originating from the neighboring porphyrin macrocycle does not cause a significant upfield shift of the phenyl protons *para* or *meta* to the bis(porphyrin)s.[45]

Thermal Studies

Thermogravimetric analyses of monoporphyrins **3** and **4** and bis(porphyrin)s **1a**, **1**, **2a**, and **2** were carried out. These six compounds were found to be thermally stable up to 150 °C, as indicated by a horizontal plateau in their TG curves. However, the mono- and bis(porphyrin)s show slightly different thermal processes. Monomers **3** and **4**, for example, exhibit similar TG curves with three obvious weight-loss processes. For **4**, the first stage, which involves the loss of a small amount of adsorbent water, four *meso*-phenyl groups, and one terminal oxygen atom, starts at 150 °C and is complete at 301.5 °C. The observed weight loss is 54.56%, in good agreement with the calculated weight loss of 54.90%. This is a continuous exothermic process. The second stage, which corresponds to the collapse of the porphyrinato skeleton, involves a strong exotherm at 373.5 °C; the process is complete at 457.8 °C. This stage leads to the stable product MoO_3 with a total weight loss of 26.16%, in agreement with the theoretical value of 26.03%. Following the second step, a medium exothermic process occurs with a further weight loss of 4.85%, thus indicating that MoO_3 is not the final product in compound **4**. According to the literature, a possible explanation for this may be the occurrence of self-heating or autocatalysis to yield a nonstoichiometric molybdenum oxide with the formula $MoO_{2.56}$.[46] In contrast to the monomers, the bis(porphyrin)s exhibit continuous decomposition processes. Figure 2 shows the TG and DTA curves for compound **2**. The decomposition of **2** starts at 150 °C and the process ends at

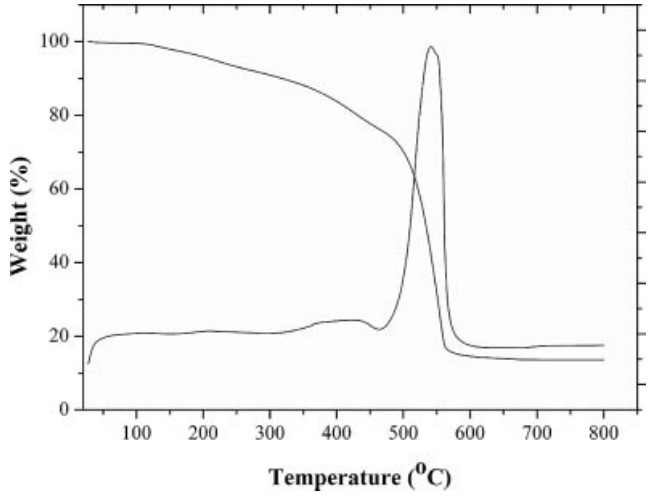

Figure 2. TG and DTA curves of compound **2**.

600 °C, as revealed by the weight loss curve. The experimental weight loss for the process is 85.57%, in good agreement with the expected value of 85.72%. This step involves the loss of a small amount of adsorbed water and the collapse of the whole porphyrin framework; the final products are expected to be MoO_3 and ZnO. Therefore, one possible reason why the yield of **2** is so low could be that Mo/Zn bis(porphyrin)s with an imidophenyl linkage are not very stable at high temperature.

Luminescence Studies

Excited-state processes in porphyrins are extremely important for their applications in molecular devices. Two fluorescence bands [S2 (B band) and S1 (Q band)] are observed in the porphyrin complexes. These are attributable to the transitions from the second excited singlet state (S2) to the ground state (S0; S2→S0) and from the lowest excited singlet state (S1) to S0 (S1→S0), respectively. The room-temperature fluorescence spectra of monomers **3** and **4** and bis(porphyrin)s **1a**, **1**, **2a**, and **2** in chloroform (1×10^{-5} M) were recorded. The excitation spectra are approximately mirror images of the absorption spectra in the Q-band region. The emission spectra obtained at an excitation wavelength of 420 nm are shown in Figure 3.[47]

The Q(0–0) fluorescence bands of these metalloporphyrin complexes are observed in the region 601–608 nm, with the Q(0–1) fluorescence bands in the region 651–655 nm, although they differ with respect to their relative intensities and fluorescent yields. It should be noted that the Q(1–0) absorption bands around 560 nm observed in the zinc tetraarylporphyrin complexes do not appear in the emission spectra of our monomer or dimers. This is probably because this band is too weak to be observed.[47] Several interesting results can be extracted from Table 3: first, the monozinc bis(porphyrin) complex **1a** has weaker Q(0–0) and more intense Q(0–1) bands than **2a**, probably due to a radiationless deactivation process. Second, the Mo/Zn porphyrin dimers **1** and **2** give almost identical fluorescence spectra, thus suggesting that the two *meso* linkages have no significant influence on the fluorescence spectra of these dimers. Third, the emission spectra of monomers **3** and **4** are obviously different, for example an intense Q(0–0) band is observed in **3** while an intense Q(0–1) band is found in **4**. The different coordination modes of the central metals are likely to be responsible for this difference − the molybdenum unit is six-coordinate while the zinc ion is only four-coordinate. Thus, the extent of spin-orbit coupling is strongly dependent on the axial ligands of the porphyrins, such as O, Cl, Br, and I. Fourth, the fluorescent yields of all six porphyrin compounds are less than 0.2, which is in accordance with those reported previously, thereby implying that the excited state S1 is primarily deactivated by radiation-less decay in porphyrins.[47] Monomers **3** and **4** give three- to five-times higher fluorescent yields than ZnTPP due to the effect of the *para*-NH_2 group on the rate of nonradiative quenching of S1 (as shown in Table 2). Furthermore, the fluorescence

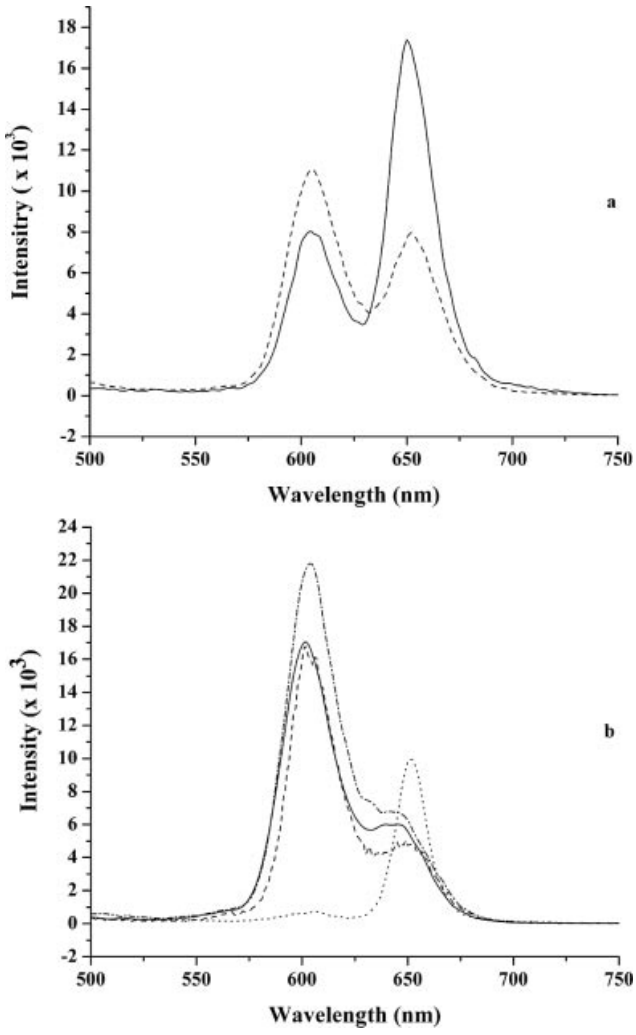

Figure 3. Emission spectra of (a) monozinc bis(porphyrin) **1a** (solid line) and **2a** (dashed line); (b) Mo-Zn porphyrin dimers **1** (solid line) and **2** (dashed line) and monomeric porphyrin complexes **3** (dash dotted line) and **4** (dotted line).

is also dependent on the coplanarity of the compounds. The coplanarity of **3** is better than that of **4**, which leads to its relatively high fluorescence yield. The fluorescent yields of bis(porphyrin)s **1a**, **2a**, **1**, and **2** are quite close to that of ZnTPP, which is due to the lack of interaction between two porphine π systems or a larger dihedral angle between the

Table 2. Emission spectra data and quantum yields (Φ_f) of the monomers and dimers.

Compounds	Q(0–0)	Q(0–1)	Φ_f
5-(*p*-NH_2)TPP		651	0.032
3	605	647	0.167
4	605	651	0.105
1a	605	650	0.043
2b	605	650	0.040
1	604	649	0.042
2	602	649	0.041
[ZnTPP][a]	598	647	0.033

[a] ZnTPP = 5,10,15,20-tetraphenylporphyrinatozinc(II).

two planes, which means that the two porphine π systems in the dimers exhibit independent fluorescence properties.

Electrochemistry

The electrochemical behavior of **1a**, **1**, **2a**, and **2** was investigated by cyclic voltammetry in dmf containing 0.1 M TEAP. The redox properties of three precursor monoporphyrinates, namely 5-(*p*-NH_2)TPP, **3**, and **4** were also studied under the same experimental conditions for comparison. The potentials were scanned positively at either +1.0 $V s^{-1}$ for 5-(*p*-NH_2)TPP, **1a**, **2**, **3**, and **4**, or at +1.25 $V s^{-1}$ for **1** and **2a**. All potentials are quoted relative to an Ag^+/Ag electrode.

As shown in Figure 4 (c), complex **4** gives a complicated cyclic voltammogram. It undergoes four reduction steps at $E_{1/2}$ = –1.86, –1.46, –1.16, and –0.43 V (vs. Ag^+/Ag; labeled as peaks I–IV). An irreversible oxidation process is also ob-

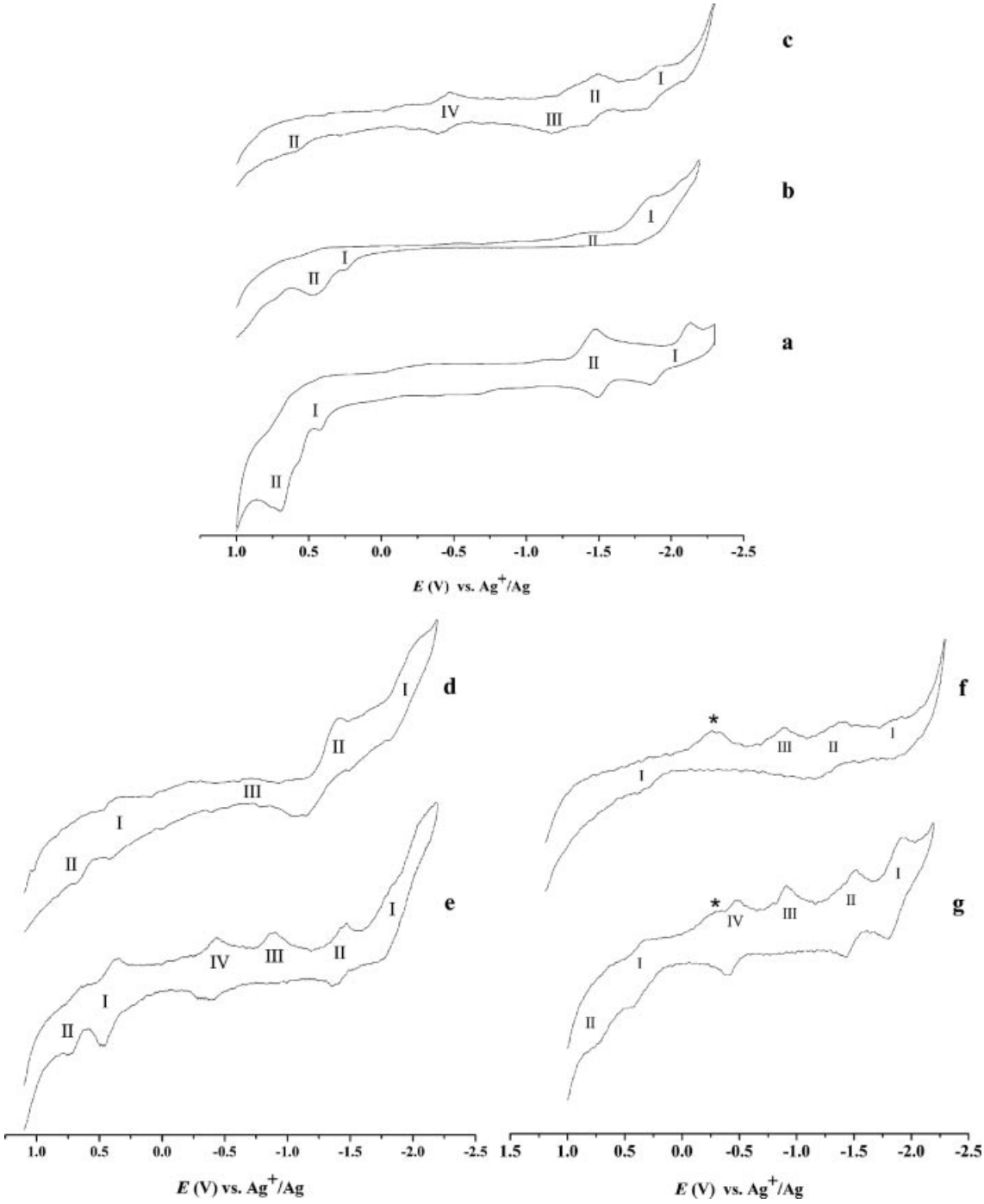

Figure 4. Cyclic voltammograms of 5-(*p*-NH_2)TPP (a), [{5-(*p*-NH_2)TPP}Zn] (**3**; b), [{5-(*p*-NH_2)TPP}$Mo^{VI}O_2$] (**4**; c), [(H_2DBPA)Zn] (**1a**; d), [{$Mo^{VI}O_2$}-DBPA-Zn] (**1**; e), [{H_2PBDA}Zn] (**2a**; f), and [{$Mo^{VI}O_2$}-PBDA-Zn] (**2**; g) in dmf + 0.1 M TEAP. The cathodic peaks marked with asterisks (*) at around –0.3 V in **2a** and **2** are due to impurities.

served at E_p = 0.51 V (vs. Ag^+/Ag). Each of these processes is a one-electron reduction or oxidation. The first two quasi-reversible reduction steps were assigned to the reductions of the central Mo (waves IV and III), namely Mo^{VI} to Mo^{V} and Mo^{V} to Mo^{IV}, while the reduction reactions occurring at the porphyrin ring (waves I and II) yield the dianion and anion radical. These reactions are shown in Scheme 2.[48] Kadish et al. have systematically investigated the electrochemistry of monomeric molybdenum porphyrins such as $[Mo^{VI}O_2(TPP)]$, $[Mo^{VI}O(TMP)(O_2)]$ (TMP = 5,10,15,20-tetramesitylporphyrinato dianion), $[Mo^{V}O(TPP)(X)]$ (X = MeO^-, OAc^-, Cl^-), $[Mo^{IV}O(TPP)]$ in dichloromethane.[30,49–54] A comparison with these molybdenum porphyrin compounds indicates that the two oxidation potentials at around 1.22 and 1.49 V (vs. SCE) in $[Mo^{VI}O_2(TPP)]$ are not observed in compound **4**, although a weak oxidation peak at 0.51 V, which is assumed to be due to the formation of the porphyrin cation radical $[Mo^{VI}O_2(por)]^{\cdot+}$, is found.[49] Furthermore, the electroreductions on the porphyrin rings of **4** in dmf are more negative than those for $[Mo^{VI}O_2(TPP)]$ in dichloromethane or 1,2-dichloroethane (–1.13 and –1.48 V vs. SCE).[54] The use of a different solvent (dmf or dichloromethane) may be the cause of this. This was further confirmed by the electrochemical behavior of the free porphyrin 5-(*p*-NH_2)TPP and the corresponding zinc complex (see parts a and b in Figure 4). [{5-(*p*-NH_2)TPP}Zn] (**3**) gives two reduction potentials at –1.81 and –1.45 V for por^-/por^{2-} and por/por^- and two oxidation potentials at 0.26 and 0.48 V for $por^{\cdot+}/por$ and $por^{\cdot2+}/por^+$, respectively. It should be noted that all three potentials related to the reductions of the porphyrin ring of **3** and **4** are shifted slightly to more positive potentials upon metalation relative the free-base porphyrin ($E_{1/2}$ = –2.00, –1.49 V). The presence of amine groups has been reported to bring about a multi-electron oxidation, particularly the potentials at 0.5–0.6 V vs. SCE that occur in H_2T(*p*-NH_2)PP in dichloromethane, although this kind of oxidation could not be distinguished in these three compounds.[54]

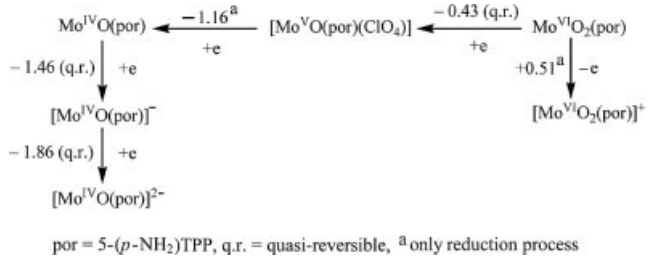

Scheme 2. The electrochemical oxidation and reduction of **4**. Values are quoted in volts.

The four bis(porphyrin) complexes **1a**, **1**, **2a**, and **2** (d–g, respectively, in Figure 4) exhibit systematic redox processes. The Mo/Zn dimers **1** and **2** exhibit similar cyclic voltammograms while the monozinc bis(porphyrin)s **1a** and **2a** also have similar properties, thus indicating that the introduction of Schiff-base or imido linkers at the periphery of porphyrins has a similar influence on their redox potential values. As seen in Table 3, the two oxidation waves at around 0.40 and 0.70 V and the two reduction waves in the ranges –1.30 to –1.45 V and –1.86 to –1.91 V correspond to the reduction of the porphyrin units in these four cases. The new totally irreversible cathodic potential at around –0.90 V that appears in the bis(porphyrin)s was assigned to the reduction of the porphyrin ligands. It is thus supposed that the increased asymmetry of bis(porphyrin)s **1a**, **2a**, **1**, and **2** may result in multiple redox processes at the porphyrin rings. Only one quasi-reversible reduction at the central metal (Mo^{VI}/Mo^{V}) is observed in **1** and **2** ($E_{1/2}$ = –0.44 V), thus indicating that further reduction from Mo^{V} to Mo^{IV} is difficult when **4** is connected to another zinc porphyrin subunit by the bridging linker.

Table 3. Half-wave potentials (V vs. Ag^+/Ag) for some porphyrin complexes in dmf containing 0.1 M TEAP as supporting electrolyte.

Ligand/complex	Reduction waves				Oxidation waves	
	I	II	III	IV	I	II
5-(*p*-NH_2)TPP	–2.00	–1.49			0.43[a]	0.70[a]
3	–1.81	–1.45[b]			0.26[a]	0.48[a]
4	–1.86	–1.46	–1.16[a]	–0.43		0.51[a]
1a	–1.91	–1.30	–0.71[b]		0.38	0.68[a]
1	–1.86	–1.45	–0.89[b]	–0.44	0.43	0.70
2a	–1.88	–1.30	–0.90[b]		0.37[a]	
2	–1.86	–1.48	–0.91[b]	–0.45	0.39	0.74[a]
$[MoO_2(TPP)]$[48]		–1.48	–1.13		1.22	1.49

[a] Only reduction process. [b] Only oxidation process.

The abstraction of an electron from Mo^{VI}, Zn^{II}, or the oxo ligand of the four bis(porphyrin) complexes is impossible, therefore the only reasonable site for oxidation is the porphyrin system; this yields the radical cations. Figure 4 (parts d–g) shows the almost identical oxidation reactions that occur at around 0.40 and 0.70 V at the porphyrin moiety, similar to those of monomeric **3** and **4**. However, these peaks are weak in comparison with those found in dichloromethane. It is noteworthy that a large decrease of the HOMO–LUMO gap, as expressed by the half-wave potential difference $E_{1/2}$(1st ox) – $E_{1/2}$(1st red), is observed for **1** and **2** (approx. 0.85 V), in comparison with the corresponding monoporphyrin complexes (approx. 1.80 V), monozinc bis(porphyrin) complexes (approx. 1.10 V), and anthracene-bridged Mo/Zn porphyrin dimer (1.27 V).[42,55] Detailed investigations of this phenomenon are currently underway.

Conclusions

We have reported the synthesis of two kinds of Mo/Zn bis(porphyrin) complexes by treating 5-(4-aminophenyl)-10,15,20-triphenylporphyrinatomolybdenum/zinc complexes with benzene-1,4-dicarbaldehyde or benzene-1,3-dicarboxylic acid. Unfortunately, we have not been able to obtain good quality single crystals for an X-ray diffraction analysis. However, we have thoroughly investigated them by

recording their electronic absorption spectra, thermal stability, luminescent spectra, and electrochemical properties. Taking into consideration previously reported Mo and Mo/Zn porphyrin complexes, we suggest that the dioxomolybdenum(VI) unit is inserted into the porphyrin ring with the two oxo groups in a *cis* configuration.

Experimental Section

Materials: Unless otherwise stated, all reagents, such as $Zn(OAc)_2 \cdot 2H_2O$, $Mo(CO)_6$, benzene-1,4-dicarbaldehyde and benzene-1,3-dicarboxylic acid, were obtained commercially and used without further purification. *N*,*N*-Dimethylformamide (dmf) for electrochemical measurement was distilled from 4 Å molecular sieves under reduced pressure before use. 5-(*p*-Aminophenyl)-10,15,20-triphenylporphyrin [5-(*p*-NH_2)TPP] and its zinc complex [{5-(*p*-NH_2)TPP}Zn] (**3**) were prepared following a literature procedure.[56–58] TEAP (tetraethylammonium perchlorate) was also obtained by the literature method.[59]

Physical and Chemical Measurements: UV/Vis spectra were recorded with a Shimadzu UV2155 spectrometer. IR spectra were measured with a Tensor 27 Fourier Transform spectrometer in the region 4000–400 cm^{-1} using KBr pellets. Elemental analyses (C,H,N) were determined with a Perkin–Elmer 2400 LSII elemental analyzer. Excitation and emission spectra were recorded with a Shimadzu PTI-600 fluorescence spectrometer at room temperature in the range from 300 to 800 nm; the quantum yields were calculated using [Zn(TPP)] as standard (Φ_f = 0.033). Molar conductances of a 1×10^{-3} M solution in chloroform at 25 °C were measured with a DDX-111A conductometer. ^{1}H NMR spectra were recorded with a Varian-Unity 500 NMR spectrometer for solutions in $CDCl_3$ with tetramethylsilane (TMS) as an internal standard. The MALDI-TOF mass spectrum for **1** was recorded with a Bruker BIFLEX III spectrometer. The ESI MS spectrum for **4** was measured with a Finnigan MATLCQ electrospray ionization-ion trap mass spectrometer. Thermogravimetric analyses (TGA) and differential thermal analyses (DTA) were performed with a thermoanalyzer (TA SDT 2960) in air at a heating rate of 10 °C min^{-1}. The redox behaviors of the complexes (ca. 1×10^{-3} M) were determined at a scan rate of 100 mV s^{-1} with an EG&G Princeton Applied Research Model 263A potentiostat/galvanostat at room temperature. An ohmic drop compensation was applied during the CV acquisition. A conventional three-electrode system was used in all electrochemical measurements, consisting of a platinum plate electrode as working electrode, a platinum-wire electrode as counter electrode, and a standard Ag^+/Ag (0.1 M $AgNO_3$ in dmf containing 0.1 M TEAP) reference electrode. The solutions were thoroughly degassed with nitrogen for at least 15 min prior to measurements.

Method 1. Preparation of [{5-(*p*-NH_2)TPP}$Mo^{VI}O_2$] (4): 5-(*p*-NH_2)TPP (200 mg, 0.32 mmol) and $Mo(CO)_6$ (200 mg, 0.76 mmol) were added to 15 mL of 1,2,4-trichlorobenzene under N_2 and the mixture was heated at 190 °C for 2 h while stirring. The progress of the reaction was monitored by UV/Vis spectroscopy. After cooling to room temperature, the solution was passed through a silica gel column (2 × 20 cm). The first band eluted with $CHCl_3$ was the free-base porphyrin. The second green band eluted with 2% $C_2H_5OH/CHCl_3$ (v:v) was collected, and the solvents evaporated to dryness to give the desired product as a brown-green powder (80.44 mg, 35%). $C_{44}H_{29}N_5MoO_2$ (755.67): calcd. C 69.93, H 3.87, N 9.27; found C 68.87, H 4.04, N 8.89. ESI-MS: *m*/*z* 757 [M + 2H]$^{2+}$. UV/Vis ($CHCl_3$): λ_{max} (ε) = 341 nm [50.7 ($\times 10^3$ $M^{-1}cm^{-1}$)], 459 (66.5), 647 (14.9). IR (KBr): $\tilde{\nu}$ = 3418 br s, (ν_{N-H}), 2953 w, 2923 m, 2853 m (ν_{C-H}), 1625 s (ν_{C-N}), 1125 w (ν_{C-O}), 946 m, 910 w (ν_{Mo-O}) cm^{-1}. ^{1}H NMR (500 MHz, $CDCl_3$): δ = 8.95 (br. s, 2 H, β-pyrrole), 8.23 (br. s, 6 H, β-pyrrole), 7.97 (br. s, 6 H, *ortho* ArH), 7.81 (br. s, 2 H^1, ArH *meta* to amido), 7.71 (dd, *J* = 4, 7 Hz, 3 H, *para* ArH), 7.54 (d, *J* = 2 Hz, 3 H, *meta* ArH), 7.05 (s, 2 H^2, ArH *meta* to amido), 4.11 (br. s, 2 H, NH) ppm.

Preparation of [{$Mo^{VI}O_2$}-DBPA-Zn] (1): [{5-(*p*-NH_2)TPP}Zn] (**3**; 37 mg, 0.053 mmol) and benzene-1,4-dicarbaldehyde (10 mg, 0.075 mmol) were dissolved in 20 mL of dmf. The solution was refluxed for 30 min while being stirred under N_2. [{5-(*p*-NH_2)-TPP}$Mo^{VI}O_2$] (50 mg, 0.053 mmol) was added to the above mixture and refluxing was continued for another 3 h. After the mixture had cooled to room temperature, the suspension was mixed with $CHC1_3$ and extracted several times with distilled water. The chloroform layer was collected and dried with anhydrous Na_2SO_4. After removal of the solvent, the residue was purified by chromatography on a neutral alumina column (2 × 10 cm) using 2% $C_2H_5OH/CHCl_3$ (v:v) as eluent to give the desired product. Recrystallization from $CHCl_3$ gave [{$Mo^{VI}O_2$}-DBPA-Zn], which was dried under vacuum to give a purple powder (46 mg, 57%). $C_{96}H_{60}MoN_{10}O_2Zn$ (1546.9): calcd. C 74.55, H 3.91, N 9.06; found C 73.18, H 3.60, N 8.68. MALDI-TOF MS: *m*/*z* 1526.0, 736.0, 692.1. UV/Vis ($CHCl_3$): λ_{max} (ε) = 337 nm [62.4 ($\times 10^3$ $M^{-1}cm^{-1}$)], 425 (285.6), 454 (68.1), 552 (29.0), 593 (13.4), 625 (7.6). IR (KBr): $\tilde{\nu}$ = 3434 m, 1697 s, 1651 s, 1523 m, 910 m, 844 w cm^{-1}. ^{1}H NMR (500 MHz, $CDCl_3$): δ = 10.14 (s, 1 H, C*H*^{3}=N), 10.00 (s, 1 H, C*H*$^{3'}$=N), 9.05 (d, *J* = 4 Hz, 2H$_\beta$, β-pyrrole), 8.96 (d, *J* = 5 Hz, 12 H$_\beta$, β-pyrrole), 8.90 (br. s, 2 H, β-pyrrole), 8.24 (br. s, 12 H, *ortho* ArH), 8.07 (d, *J* = 8 Hz, 2 H^1 and 2 H$^{1'}$, ArH *meta* to Schiff base), 7.86 (d, *J* = 8 Hz, 6 H, *para* ArH), 7.76 (s, 12 H, *meta* ArH), 7.69 (br. s, 2 H^2 and 2 H$^{2'}$, ArH *para* to Schiff base), 7.53 (br., 2 H^4, bridge-phenyl), 7.50 (d, *J* = 8 Hz, 2 H^5, bridge-phenyl) ppm.

Preparation of [{$Mo^{VI}O_2$}-PBDA-Zn] (2): [{5-(*p*-NH_2)TPP}Zn] (30 mg, 0.043 mmol) and benzene-1,3-dicarboxylic acid (12 mg, 0.072 mmol) were dissolved in 20 mL of dmf and the solution was refluxed for 30 min under N_2. [{5-(*p*-NH_2)TPP}MoO_2] (**4**; 28 mg, 0.039 mmol) was then added to the reaction solution and reflux was continued for another 3 h. After the mixture had cooled to room temperature the suspension was poured into 70 mL of $CHC1_3$ and extracted three times with distilled water. The chloroform layer was collected and dried with anhydrous Na_2SO_4. After the removal of the solvent, the residue was purified by chromatography on a neutral alumina column (2 × 10 cm) using 2% $C_2H_5OH/CHCl_3$ (v:v) as eluent to afford the desired product, which was dried under vacuum to give a purple powder (44 mg, 59%). $C_{96}H_{60}MoN_{10}O_4Zn$ (1578.9): calcd. C 73.04, H 3.80, N 8.88; found C 72.38, H 4.15, N 8.11. UV/Vis ($CHCl_3$): λ_{max} (ε) = 340 nm [59.8 ($\times 10^3$ $M^{-1}cm^{-1}$)], 424 (293.8), 458 (89.5), 553 (24.1), 590 (14.5), 626 (9.7). IR (KBr): $\tilde{\nu}$ = 3434 s, 1652 m, 1620 br. s, 1520 s, 951 br m, 875 br w, cm^{-1}. ^{1}H NMR (500 MHz, $CDCl_3$): δ = 10.30 (br. s, 2 H, O=C–N*H*^{3}–), 8.95 (m, 12 H$_\beta$, β-pyrrole), 8.84 (br. s, 4 H$_\beta$, β-pyrrole), 8.231 (d, *J* = 6 Hz, 12 H, *ortho* ArH), 7.99 (s, 1 H^4, bridge-phenyl), 7.94 (br., 2 H^1, ArH *meta* to imido), 7.88 (d, *J* = 5 Hz, 2 H^5, bridge-phenyl), 7.75 (br. s, 8 H, *meta* ArH), 7.62 (m, 4 H, *meta* ArH), 7.53 (t, *J* = 6 Hz, 6 H, *para* ArH), 7.46 (t, *J* = 8 Hz, 1 H^6, bridge-phenyl), 7.18 (m, 2 H$^{1'}$, ArH *meta* to imido), 6.91 (d, *J* = 3 Hz, 2 H^2, ArH *ortho* to imido), 6.64 (br., 2 H$^{2'}$, ArH *ortho* to imido) ppm.

Method 2. Preparation of [(H_2DBPA)Zn] (1a): 5-(*p*-NH_2)TPP (200 mg, 0.32 mmol) and benzene-1,4-dicarbaldehyde (50 mg, 0.37 mmol) were added to 30 mL of dmf and the mixture was re-

fluxed for 30 min under N_2. [{5-(*p*-NH_2)TPP}Zn] (220 mg, 0.32 mmol) was then added and the reflux was maintained for another 3 h, during which time the process was monitored by UV/Vis spectroscopy every 10 min. After cooling to room temperature, 70 mL of $CHC1_3$ was poured into the solution and this mixture extracted several times with distilled water. The $CHCl_3$ layer was collected, dried with anhydrous Na_2SO_4, filtered to remove the drying agent, and finally evaporated to a small volume. The crude product was purified by chromatography on a neutral alumina column (3.0 × 10 cm). The first band, which eluted with $CHCl_3$, was unreacted [{5-(*p*-NH_2)TPP}Zn]. The main purple band, which eluted with 2% $C_2H_5OH/CHCl_3$ (v:v), was collected and condensed to dryness on a rotary evaporator to afford the desired product (108 mg, 24%). $C_{96}H_{62}N_{10}Zn$ (1421.0): calcd. C 81.14, H 4.40, N 9.86; found C 79.98, H 4.55, N 8.97. UV/Vis ($CHCl_3$), λ_{max} (ε): 429 nm [269.3 (10^3 м$^{-1}$ cm^{-1})], 517 (18.3), 554 (27.3), 595 (12.5), 648 (4.9). IR (KBr): $\tilde{\nu}$ = 3430 s, 1659 m, 1628 s, 1550 m, 963 m cm^{-1}. ^{1}H NMR (500 MHz, $CDCl_3$): δ = 10.16 (s, 2 H, C*H*^{3}=N–), 9.02 (br., 2 H_β, β-pyrrole), 8.95 (d, *J* = 9 Hz, 4 H_β, β-pyrrole), 8.85 (d, J = 5 Hz, 4 H_β, β-pyrrole), 8.64–8.58 (br., 6 H_β, β-pyrrole), 8.23 (br. s, 12 H, o*rtho* ArH), 8.08 (d, *J* = 9 Hz, 4 H^1, ArH, *meta* to Schiff base), 7.89 (d, *J* = 8 Hz, 6 H, *para* ArH), 7.77 (d, *J* = 7 Hz, 12 H, *meta* ArH), 7.63 (d, *J* = 6 Hz, 4 H^2, ArH, *para* to Schiff base), 7.57 (d, *J* = 7 Hz, 2 H^4, bridge-phenyl), 7.53 (d, *J* = 9 Hz, 2 H^5, bridge-phenyl), –2.75 (s, 2 H, N–H) ppm.

Preparation of [(H_2PBDA)Zn] (2a): 5-(*p*-NH_2)TPP (200 mg, 0.32 mmol) and benzene-1,3-dicarboxylic acid (60 mg, 0.36 mmol) were added to 30 mL of dmf and the mixture was refluxed for 30 min under N_2. [{5-(*p*-NH_2)TPP}Zn] (**3**; 220 mg, 0.32 mmol) was then added and the mixture was refluxed for another 3 h, during which the process was monitored by UV/Vis spectroscopy every 10 min. After cooling to room temperature, 70 mL of $CHC1_3$ was poured into the solution and the mixture extracted several times with distilled water. The $CHCl_3$ layer was collected, dried with anhydrous Na_2SO_4, filtered to remove the drying agent, and finally evaporated to a small volume. The crude product was purified by chromatography on a neutral alumina column (2× 10 cm). The first band, which eluted with $CHCl_3$, was unreacted [{5-(*p*-NH_2)-TPP}Zn]. The main purple band, which eluted with 2% $C_2H_5OH/CHCl_3$ (v:v), was collected and the solvents evaporated to dryness to obtain the desired product (164 mg, 35%). $C_{96}H_{62}N_{10}O_2Zn$ (1453.0): calcd. C 79.35, H 4.30, N 9.64; found C 77.97, H 3.98, N 9.17. UV/Vis ($CHCl_3$): λ_{max} (ε) = 428 nm [277.1 (10^3 м$^{-1}$ cm^{-1})], 519 (17.2), 554 (26.0), 594 (11.8), 650 (4.9). IR (KBr): $\tilde{\nu}$ = 3380 m, 1652 s, 1635 s, 1532 m, 966 w cm^{-1}. ^{1}H NMR (500 MHz, $CDCl_3$): δ = 10.27 (br. s, 2 H, O=C–N*H*^{3}–), 8.87–8.83 (br., 12 H, β-pyrrole), 8.81–8.80 (br., 4 H_β, β-pyrrole), 8.21 (d, *J* = 6 Hz, 12 H, *ortho* ArH), 8.01 (s, 2 H^4, bridge-phenyl), 7.95 (d, *J* = 7 Hz, 2 H^5, bridge-phenyl), 7.93 (br. s, 4 H^1, *meta* ArH), 7.74 (t, *J* = 6 Hz, 12 H, *meta* ArH), 7.53 (t, *J* = 6 Hz, 6 H, *para* ArH), 6.91 (br., 4 H^2, ArH *ortho* to imido), –2.75 (s, 2 H, N–H) ppm.

Preparation of [{$Mo^{VI}O_2$}-DBPA-Zn] (1): [(H_2DBPA)Zn] (**1a**; 50 mg, 0.035 mmol) and $Mo(CO)_6$ (50 mg, 0.190 mmol) were added to 10 mL of 1,2,4-trichlorobenzene and the mixture was refluxed while stirring for 4 h under N_2. The progress of the reaction was monitored by UV/Vis spectroscopy. After cooling to room temperature, the solution was transferred directly onto a neutral alumina column (2 × 10 cm). The first red band, which eluted with $CHCl_3$, was unreacted [(H_2DBPA)Zn]. The second purple-red band, which eluted with 2% $C_2H_5OH/CHCl_3$ (v:v), was collected and the solvents evaporated to dryness to give the desired product (23 mg, 42%).

Preparation of [{$Mo^{VI}O_2$}-PBDA-Zn] (2): [(H_2PBDA)Zn] (50 mg, 0.035 mmol) and $Mo(CO)_6$ (50 mg, 0.190 mmol) were added to 10 mL of 1,2,4-trichlorobenzene and the mixture was refluxed while stirring for 4 h under N_2. The progress of the reaction was monitored by UV/Vis spectroscopy. After cooling to room temperature, the solution was transferred directly onto a neutral alumina column (2 × 10 cm). The first red band, which eluted with $CHCl_3$, was unreacted [(H_2PBDA)Zn]. The second purple-red band, which eluted with 2% $C_2H_5OH/CHCl_3$ (v:v), was collected and the solvents evaporated to dryness to give the desired product (10 mg, 5.5%).

Acknowledgments

We would like to thank the Jilin University Youth Foundation for financial support. The permanent, generous support of Prof. Guo-Fa Liu and Prof. Qing-Bo Meng is gratefully acknowledged.

[1] O. Siri, L. Jaquinod, K. M. Smith, *Tetrahedron Lett.* **2000**, *41*, 3583–3587.
[2] T.-G. Zhang, Y. Zhao, I. Asselberghs, A. Persoons, K. Clays, M. J. Therien, *J. Am. Chem. Soc.* **2005**, *127*, 9710–9720.
[3] J. P. Collman, J. M. Garner, *J. Am. Chem. Soc.* **1990**, *112*, 166–173.
[4] H. Mizuseki, R. V. Belosludov, A. A. Farajian, N. Igarashi, Y. Kawazoe, *Mater. Sci. Eng., C* **2005**, *25*, 718–721.
[5] T. Morotti, M. Pizzotti, R. Ugo, S. Quici, M. Bruschi, P. Mussini, S. Righetto, *Eur. J. Inorg. Chem.* **2006**, 1743–1757.
[6] J. Jiao, F. Anariba, H. Tiznado, I. Schmidt, J. S. Lindsey, F. Zaera, D. F. Bocian, *J. Am. Chem. Soc.* **2006**, *128*, 6965–6974.
[7] Q. Wang, W. M. Campbell, E. E. Bonfantani, K. W. Jolley, D. L. Officer, P. J. Walsh, K. Gordon, R. Humphry-Baker, M. K. Nazeeruddin, M. Gratzel, *J. Phys. Chem. B* **2005**, *109*, 15397–15409.
[8] L. Schmidt-Mende, W. M. Campbell, Q. Wang, K. W. Jolley, D. L. Officer, M. K. Nazeeruddin, M. Gratzel, *ChemPhysChem.* **2005**, *6*, 1253–1258.
[9] S. Cherian, C. C. Wamser, *J. Phys. Chem. B* **2000**, *104*, 3624–3629.
[10] C. A. Hunter, S. Tomas, *J. Am. Chem. Soc.* **2006**, *128*, 8975–8979.
[11] M. O. Senge, *Chem. Commun.* **2006**, 243–256.
[12] R. S. Loewe, R. K. Lammi, J. R. Diers, C. Kirmaier, D. F. Bocian, D. Holten, J. S. Lindsey, *J. Mater. Chem.* **2002**, *12*, 1530–1552.
[13] C. J. Byrne, M. A. Cooper, P. A. Cowled, R. Johnstone, L. Mackenzie, L. V. Marshallsay, I. K. Morris, C. A. Muldoon, M. J. Raftery, S. S. Yin, A. D. Ward, *Austr. J. Chem.* **2004**, *57*, 1091–1102.
[14] M. Schaffer, P. M. Schaffer, L. Corti, M. Gardiman, G. Sotti, A. Hofstetter, G. Jori, E. Duhmke, *J. Photochem. Photobiol., B* **2002**, *66*, 157–164.
[15] J. Borowiec, I. Trojnar, S. Wolowiec, *Polyhedron* **2004**, *23*, 33–39.
[16] S. Faure, C. Stern, R. Guilard, P. D. Harvey, *Inorg. Chem.* **2005**, *44*, 9232–9241.
[17] H. Shinmori, T. K. Ahn, H. S. Cho, D. Kim, N. Yoshida, A. Osuka, *Angew. Chem. Int. Ed.* **2003**, *42*, 2754–2758.
[18] K. Susumu, T. Shimidzu, K. Tanaka, H. Segawa, *Tetrahedron Lett.* **1996**, *37*, 8399–8402.
[19] J. P. Collman, S. T. Harford, S. Franzen, J.-C. Marchon, P. Maldivi, A. P. Shreve, W. H. Woodruff, *Inorg. Chem.* **1999**, *38*, 2085–2092.
[20] J. P. Collman, S. T. Harford, S. Franzen, A. P. Shreve, W. H. Woodruff, *Inorg. Chem.* **1999**, *38*, 2093–2097.
[21] E. Malinowska, J. Niedziolka, E. Rozniecka, M. E. Meyerhoff, *J. Electroanal. Chem.* **2001**, *514*, 109–117.

[22] P. D. Harvey, N. Proulx, G. Martin, M. Drouin, D. J. Nurco, K. M. Smith, F. Bolze, C. P. Gros, R. Guilard, *Inorg. Chem.* **2001**, *40*, 4134–4142.
[23] S. Faure, C. Stern, R. Guilard, P. D. Harvey, *Inorg. Chem.* **2005**, *44*, 9232–9241.
[24] J. P. Collman, P. Denisevich, Y. Konai, M. Marrocco, C. Koval, F. C. Anson, *J. Am. Chem. Soc.* **1980**, *102*, 6027–6036.
[25] Y. Matsuda, Y. Murakami, *Coord. Chem. Rev.* **1988**, *92*, 157–192.
[26] H. Brand, J. Arnold, *Coord. Chem. Rev.* **1995**, *140*, 137–168.
[27] T. S. Srivastava, E. B. Fleischer, *J. Am. Chem. Soc.* **1970**, *92*, 5518–5519.
[28] T. Fujihara, Y. Sasaki, T. Imamura, *Chem. Lett.* **1999**, 403–404.
[29] T. Fujihara, N. H. Rees, K. Umakoshi, J. Tachibana, U. Sasaki, W. McFarlane, T. Imamura, *Chem. Lett.* **2000**, 102–103.
[30] T. Fujihara, K. Myougan, A. Ichimura, Y. Sasaki, T. Imamura, *Chem. Lett.* **2001**, 178–179.
[31] J. P. Collman, P. S. Wagenknecht, J. E. Hutchison, *Angew. Chem. Int. Ed. Engl.* **1994**, *33*, 1537–1554.
[32] T. Haino, T. Fujii, Y. Fukazawa, *J. Org. Chem.* **2006**, *71*, 2572–2580.
[33] M. Takeuchi, S. Tanaka, S. Shinkai, *Chem. Commun.* **2005**, 5539–5541.
[34] K. Ogawa, A. Ohashi, Y. Kobuke, K. Kamada, K. Ohta, *J. Am. Chem. Soc.* **2003**, *125*, 13356–13357.
[35] J. Borowiec, I. Trojnar, S. Wolowiec, *Polyhedron* **2004**, *23*, 33–39.
[36] W. J. Geary, *Coord. Chem. Rev.* **1971**, *7*, 81–122.
[37] S. O. Grim, L. J. Matienzo, *Inorg. Chem.* **1975**, *14*, 1014–1018.
[38] J.-Q. Xu, X.-H. Zhou, L.-M. Zhou, T.-G. Wang, B. A. Averill, *Inorg. Chim. Acta* **1999**, *285*, 152–154.
[39] M. Nappa, J. S. Valentine, *J. Am. Chem. Soc.* **1978**, *100*, 5075–5080.
[40] E. Deiters, V. Bulach, M. W. Hosseini, *New J. Chem.* **2006**, *30*, 1289–1294.
[41] T. Morotti, M. Pizzotti, R. Ugo, S. Quici, M. Bruschi, P. Mussini, S. Righetto, *Eur. J. Inorg. Chem.* **2006**, 1743–1757.
[42] T. Fujihara, K. Tsuge, Y. Sasaki, Y. Kaminaga, T. Imamura, *Inorg. Chem.* **2002**, *41*, 1170–1176.
[43] H. J. Ledon, M. C. Bonnet, Y. Brigandat, F. Varescon, *Inorg. Chem.* **1980**, *19*, 3488–3491.
[44] H. J. Ledon, M. C. Bonnet, J.-Y. Lallemand, *J. Chem. Soc., Chem. Commun.* **1979**, 702–704.
[45] S. Wolowiec, *Polyhedron* **1998**, *17*, 1295–1301.
[46] M. I. Diaz-Guemes, *Thermochim. Acta* **1986**, *106*, 125–132.
[47] D. J. Quimby, F. R. Longo, *J. Am. Chem. Soc.* **1975**, *97*, 5111–5117.
[48] T. Malinski, P. M. Hanley, K. M. Kadish, *Inorg. Chem.* **1986**, *25*, 3229–3235.
[49] J.-H. Fuhrhop, K. M. Kadish, D. G. Davis, *J. Am. Chem. Soc.* **1973**, *95*, 5140–5147.
[50] T. Malinski, H. Ledon, K. M. Kadish, *J. Chem. Soc., Chem. Commun.* **1983**, 1077–1079.
[51] H. Ledon, F. Varescon, F. Varescon, T. Malinski, K. M. Kadish, *Inorg. Chem.* **1984**, *23*, 261–263.
[52] Y. Matsuda, S. Yamada, Y. Murakami, *Inorg. Chem.* **1981**, *20*, 2239–2246.
[53] K. M. Danish, T. Malinski, H. Ledon, *Inorg. Chem.* **1982**, *21*, 2982–2987.
[54] A. Bettelheim, B. A. White, S. A. Raybuck, R. W. Murray, *Inorg. Chem.* **1987**, *26*, 1009–1017.
[55] P. Bhyrappa, M. Sankar, B. Varghese, *Inorg. Chem.* **2006**, *45*, 4136–4149.
[56] D.-M. Li, Z.-X. Zhao, S.-Q. Liu, G.-F. Liu, T.-S. Shi, X.-X. Liu, *Synth. Commun.* **2000**, *30*, 4017–4026.
[57] W. J. Kruper Jr, T. A. Chamberlin, M. Kochanny, *J. Org. Chem.* **1989**, *54*, 2753–2756.
[58] A. D. Alder, F. R. Longo, V. Varadi, *Inorg. Synth.* **1976**, *16*, 213–220.
[59] H. O. House, E. Feng, N. P. Peet, *J. Org. Chem.* **1971**, *36*, 2371–2375.

Received: September 13, 2006
Published Online: March 13, 2007

